Light Metals 2012 *Edited by: Carlos E. Suarez*
TMS (The Minerals, Metals & Materials Society), 2012

STUDY ON MECHANICAL PROPERTIES OF 2024 AL SHEET TREATED BY SMAT AND HOT/COLD ROLLING

Ka-Po Cheung[1], San-Qiang Shi[1] and Jian Lu*[2]
[1]Department of Mechanical Engineering, The Hong Kong Polytechnic University, 1 Yuk Choi Road, Hung Hom, Hong Kong, China
[2]Department of Manufacturing Engineering and Engineering Management, City University of Hong Kong, 83 Tat Chee Avenue, Kowloon, Hong Kong, China

Keywords: Aluminum alloy, Surface Mechanical Attrition Treatment, Tensile properties

Abstract

The strengthening effects of hot/cold rolling and surface mechanical attrition treatment (SMAT) on aluminium alloy were investigated in this paper. Before performing the rolling processes, aluminium sheets were treated using SMAT on both sides for 40 min at room temperature. The parameters for the hot/cold rolling process included a range of operating temperatures (-200 °C to 480 °C) and percentages of thickness reduction (up to 85%). Then the mechanical properties of rolled samples of different thicknesses were studied. Tensile test results showed that the higher the percentage of reduction in thickness, the higher the strength of the rolled samples that could be obtained. Considering the yield and tensile strength, rolling at room temperature with 80% thickness reduction was the optimum condition for AA2024-T3 in this article, in which the yield and ultimate tensile strength were increased by 54% and 79% respectively. It was also found that the ductility was also enhanced according to the operating temperature.

Introduction

The selection and design of modern high-performance structural engineering materials is driven by optimizing combinations of mechanical properties such as strength, ductility, toughness and elasticity [1]. 2000 series wrought aluminium-copper alloys are commonly used for aerospace applications because of their light weight and comparable strengths to steel. The material thus employed in this investigation is the Aluminium alloy *Al-Cu-Mn-Mg* in plate form with the T3 temper (hereafter AA2024-T3). AA2024-T3, as a material with high strength but low density, has been widely used in the engineering industries, especially in the aviation industry in recent years.

Surface nanocrystallization (SNC) is expected to produce nanocrystalline materials on the surface layer and to improve the properties of engineering materials. Surface mechanical attrition treatment (SMAT) [2, 3] has recently become an important aspect of a surface treatment in the industry to improve the performance of metallic parts subjected to fatigue loading or stress corrosion [4]. The basic principle of SMAT is the repeated multidirectional impacts of accelerated metallic or ceramic spheres at high strain rates onto the surface layer of a bulk metal. This results in severe plastic deformation with a gradient of grain refinement along the deformation depth [5]. This technique produces surface nanocrystalline layers in bulk materials, which enhances the surface hardness and corrosion resistance [6, 7]. The reduction of grain size is known to have a significant enhancement effect on the mechanical properties of materials [8]. This technique has been effectively used to achieve surface nanocrystallization with a mean grain size of 10 to 50 nm in a variety of pure metals and alloys [5, 9-11]. These SNC treated materials display superior mechanical properties compared to those of untreated materials. With the use of ceramic spheres, it is expected that the mechanical properties of aluminium alloys will be significantly enhanced after the SMAT process without any change in chemical composition [12]. In addition, owing to its low cost and the availability of comparatively large scale production, SMAT is a favourable synthesis method for commercially affordable nanostructures.

Aluminium has a complex material response due to strengthening. The nature of the interaction mechanisms between mobile dislocations and obstacles such as solute, precipitates, and forest dislocations has drawn much interest from scholars. Processes of deformation at high temperature relying on constitutive models have often been cited as one of the essential elements which have contributed to the kinetics of metal plasticity [13].

Some of the research shows that the materials are refined with ultrafine grains and highly strengthened [14-18] due to the severely deformed region occurring both on the surface and in the interior region. Large volume fraction of equiaxed regions intermixed with lamellar regions show orientations corresponding to the rolling or shear texture components [19]. Extensive comparison between cyclic testing and the more routine monotonic compressive loading procedures establishes that the incremental step test is an expedient means of surveying the kinetics of plastic flow. The quality is influenced by a number of interdependent parameters such as processing temperature, pressure (determined by the level of thickness reduction) and contact time (roll speed) [20-22]. Hence, the optimizations for the strengthening process parameters are still world-wide challenges for researchers. In general, an increase in rolling temperature may result in a higher yield and tensile strength for rolled materials. However, the issue regarding how rolling aluminium alloy at warm temperature after the SMAT process affects the mechanical properties is not well understood.

To reduce the concept to practice, we adapt the techniques of SMAT and warm rolling to fabricate a nanocrystalline surface layer with strengthening effect on AA2024-T3. The tensile properties of aluminium alloy will be studied. The effects of the SMATed layer and the rolling process on the microstructure of the base alloy are further investigated by XRD and SEM.

Experimental Process

1. Materials

AA2024-T3 aluminium sheets with 2.5 mm in thickness were selected for the experiment. This aluminium alloy is essentially composed of 92.7% Al, 4.4% Cu, 1.33% Mg and 0.62% Mn. The yield strength of the as-received material is 370 MPa, the Young's modulus 73,100 MPa and the Poisson's ratio 0.34. The specimens were cut into pieces with the dimension of 70 mm × 50 mm × 2.5 mm for further investigation.

2. SMAT

SMAT can induce grain refinement at the nanometer scale in the surface layer of bulk samples by generating the plastic deformation in the top surface layer [6, 23]. The plastic deformation in the surface layer with a large strain and a high strain rate results in a progressive refinement of coarse grains into the nanometer regime. This nanocrystalline surface layer forms due to large grain boundary misorientations, dislocation blocks and microbands [5]. Ceramic balls (with a diameter of 3 mm) are filled in a cylinder-shaped vacuum chamber attached to a vibration generator. Due to the applied high vibration frequency of the system (20 kHz), the sample surface under treatment will be bombarded repetitively by a large number of balls within a short duration, resulting in a severely plastically deformed sample surface layer. Part of the samples were SMATed on both sides for 40 min. Ceramic spheres were chosen for the SMAT process instead of stainless steel in this case. The possibility of Fe contamination on the sample surfaces can be eliminated, though the energy acting on the samples will be smaller [24].

3. Rolling

After performing the SMAT process, the AA2024-T3 sheets were either preheated in a range of temperatures (200 °C (P), 380 °C (T) and 480 °C (F)) for 40 min in an oven, or immersed into liquid nitrogen (-200 °C (LN)) for 2 min. The sheets were deformed by rolling to achieve a specific reduction in the sample thickness and the mechanical properties of rolled samples with different thicknesses will then be studied. The two digits indicate the percentage of the thickness reduction, and the letter 'S' indicates the specimen was SMATed before the rolling process. The samples were rolled at a constant speed of 25m/min. To reduce the tendency of cracking, the reduction of the thickness for the sheets is around 10% per each roll. After each pass, the sheets were kept in either the oven or the liquid nitrogen bath accordingly for over 2 min before the next reduction.

4. Characterization of Mechanical Properties

XRD Spectroscopy is a non-destructive method to characterise the crystal structure of various materials in bulk solids, powders or thin film form. It has been broadly used to investigate the structural qualities of thin sheets. Crystal orientation, distribution and residual stress were analysed for the phase identification by using the Philips Xpert XRD System and the Bruker AXS D8 DISCOVER. X-ray diffraction patterns of the SMATed and rolled samples were collected. The samples were examined with Co-Kα_1 radiation (λ = 1.789 Å) in continuous scanning mode over aθ2 angle of 20° – 120° at a step of 0.02°/s.

The specimens for uni-axial tensile test were scaled down and machined according to the specification of ASTM standards B-557M. The gauge dimension of the samples is 34 mm x 6 mm along the rolling direction. The tensile tests were conducted at ambient temperature under the strain rate of 2 x 10^{-4} /s and displacement rate of 1 mm/min. All the tensile tests were done on a standard testing machine (tensile machine: 50 kN MTS Alliance RT-50; extensometer: MTS 632 24F-50). The yield strength (σ_{YS}), ultimate tensile strength (σ_{UTS}) and elongation at breaks (ε_{BREAK}) of the specimen were then obtained.

Fractured cross-section morphologies of the samples after the tensile tests were further inspected in SEM (JEOL 6490). The chemical composition and element distribution on the cross-section area were analysed by EDS.

Results and discussion

As the hot rolling process is capable of further enhancing the mechanical properties of the treated materials, it is applied to AA2024 of 2.5 mm thickness in this work. This material is chosen owing to its sufficient thickness, which is susceptible to being rolled. The parameters of the hot rolling process are studied in order to obtain the optimum conditions. The reduction of the sheet thickness is around 10% per roll.

1. Tensile tests

Figures 1a to e are the tensile test results of the AA2024 sheets with thickness of 2.5 mm, which were rolled at -20 °C (LN), room temperature (RT), 200 °C (P), 380 °C (T) and 480 °C (F), respectively. Those samples rolled at room temperature or under cryogenic conditions have similar strength. For the samples rolled at the same temperature, the higher the percentage of thickness reduction, the higher the strength of the rolled samples in most cases. The outcome of the elongation is completely opposite to the strength results, as the trend shows that the higher the percentage of thickness reduction, the lower the ductility of the metal sheets are obtained. It is apparent that the ductility is not so temperature dependent. No clear trend can be observed between elongation and rolling temperature.

The yield stress profiles of LN60 and LN80 show similar behaviours, though the ultimate tensile stress profile is more contrasted (Figure 2a), due to the reduction in the strain hardening capacity. Considering the tensile strength results of all the conditions, rolling at room temperature with the 80% thickness reduction may be the optimum conditions for AA2024. Maximum tensile strength of the whole process is recorded in this case, in which the yield and ultimate tensile strength have been increased by 54% and 79% respectively (Figure 2b). This causes the material to become brittle. The moderate enhancement in yield strength can be attributed to the grain refinement and the introduction of dislocations. The profile of strength and elongation in Figure 2c is relatively similar to Figure 2b, which also shows the comparable trend that the higher the percentage of the thickness reduction, the higher the strength that can be obtained.

In order to obtain the rolled materials with both desirable yield strength and ductility, it is found that rolling at 380 °C with 50% thickness reduction is a remarkable process combination (Figure 2d). It is plausible that the fragmentation of grains occurred during the hot rolling process with 50% thickness reduction, which induced the dislocation between the small grains; hence the value of the ultimate tensile strength achieved is the highest among those hot-rolled samples. The corresponding strength profile is almost constant in Figure 2f, only a greater drop in elongation was observed for specimens with 20% thickness reduction. Both yield and ultimate tensile strength are lower than the as-received specimens. It has to be pointed out that recrystallization can occur at the annealing temperature of 413 °C for AA2024-T3 and it can erase the former history of the precipitation treatment.

In the present materials, the peak stress indicates the occurrence of tensile instability. This means that the nucleated microcrack in the nanostructured layer starts advancing and causes a drop in tensile stress. However, this tensile instability is non-localized and does not cause the complete rupture of the materials; in contrast, it

delays the final failure and makes the materials tougher due to the initiation of cracks in other locations.

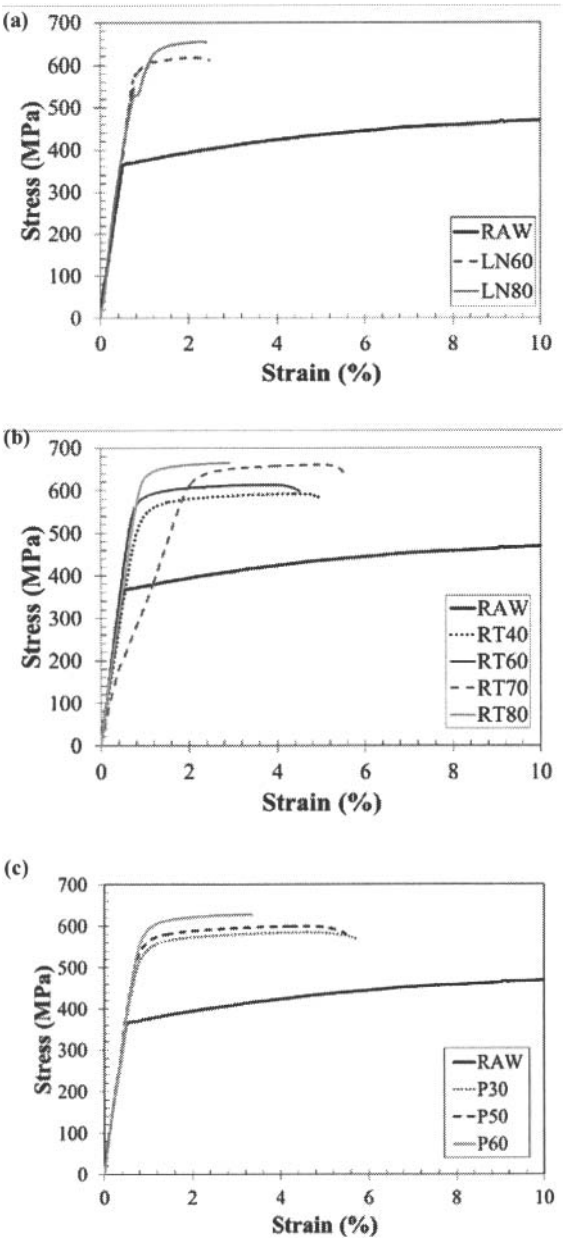

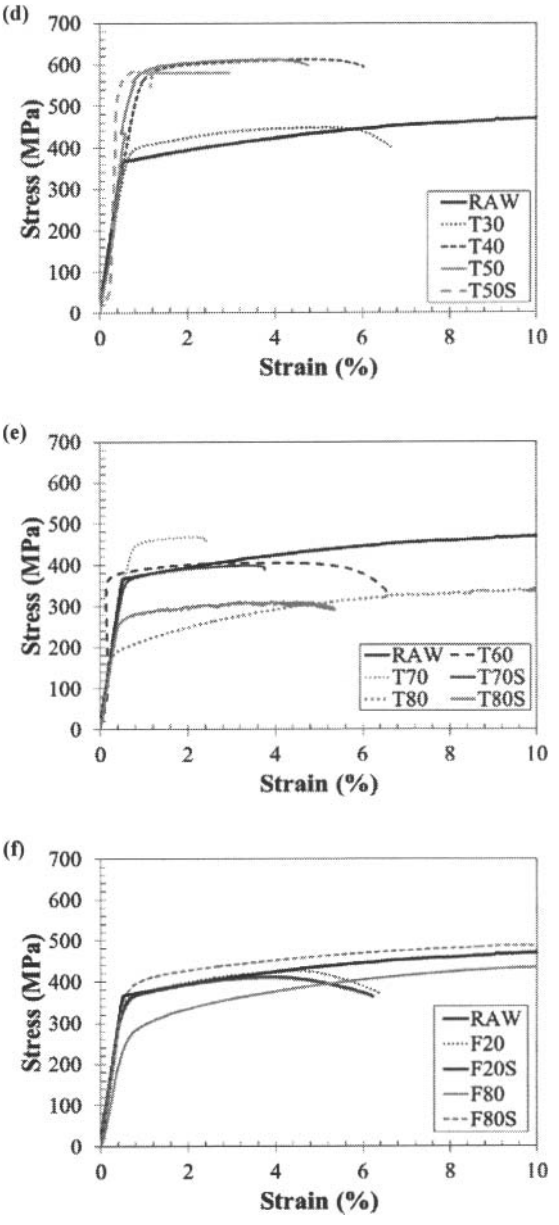

Figure 1. Engineering stress-strain curves of the rolled and SMATed specimens at (a) -200 °C, (b) room temperature, (c) 200 °C, (d) and (e) 380 °C, and (f) 480 °C, comparing with the as-received samples.

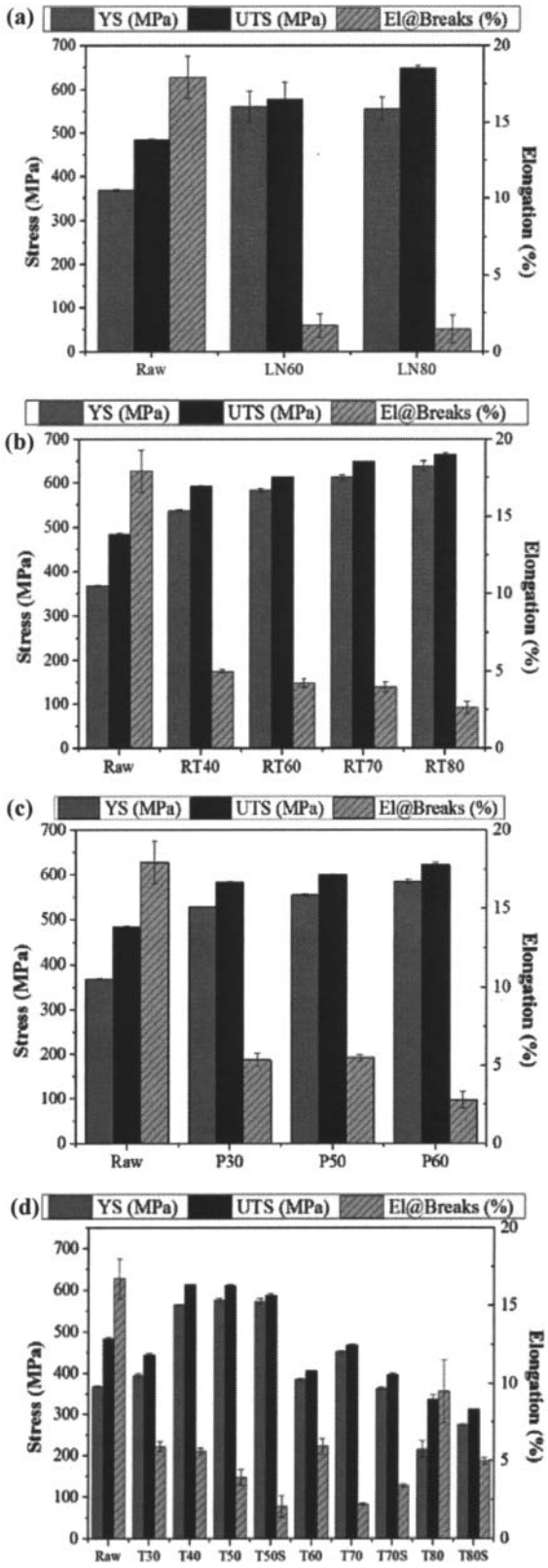

Figure 2. Profiles of yield stress (YS), ultimate tensile stress (UTS) and elongation obtained by tensile tests for the rolled and SMATed specimens at (a) -200 °C, (b) room temperature, (c) 200 °C, (d) 380 °C and (e) 480 °C.

2. Microstructure of nanocrystalline layer

2.1. XRD. The physical change of metals on the surface layer after hot rolling and SMAT can be studied through XRD. This can be used to carry out residual stress analysis and texture analysis. Figure 3 displays the XRD patterns of the SMATed and rolled samples indicating the location of Bragg-diffraction peaks and full width at half maximum (FWHM), compared with the untreated one. The FWHM values at (1 1 1), (2 0 0), (2 2 0), (3 1 1) and (2 2 2) peaks of the as-received aluminium are 0.52, 0.42, 0.46, 0.50 and 0.57, respectively. The values of rolled specimens are 0.75, 0.46, 0.53, 0.63 and 0.62 respectively while the specimens treated by both SMAT and rolling are 0.62, 0.45, 0.88, 0.64 and 0.56 respectively. The difference in values is due to the grain refinement. According to the Scherrer equation [25], the average grain size of the rolled specimen surfaces has decreased by 18%, and those treated by both SMAT and rolling has decreased by 10%, compared to the as-received specimens.

It is noted that SMAT does not result in any phase transformation; however, the diffraction peaks of the SMATed sample are apparently broadened, indicating that the non-uniform strain is acting on the specimen and the grains on the XRD-detected layer are refined. The peak profile is a convolution of the profiles from all of these contributions. XRD intensity of metal decreases gradually when grain size of the metal decreases.

X-ray diffraction peak shifts are found in those diagrams due to refraction in these strong asymmetric diffraction geometries, which indicates the different types of internal stresses and planar faults, especially stacking faults or twin boundaries [26]. No additional peaks are found after both treatments, from which it can be concluded that no contamination at surface of 2024 Al alloy is from SMAT process.

2.2. SEM Fractography. The cross-sectional optical microstructure of the specimens which annealed at 340 °C and rolled with a thickness reduction of 50% are shown in Figure 4. The SEM diagrams show that the gradient structure resulting from a gradual decrease in the applied strain with increasing depth of the deformed layer was found, which represents the complete range of the structure changes during the treatment. The coarse grains in the undeformed region are about 50 μm in width and 100–200 μm in length.

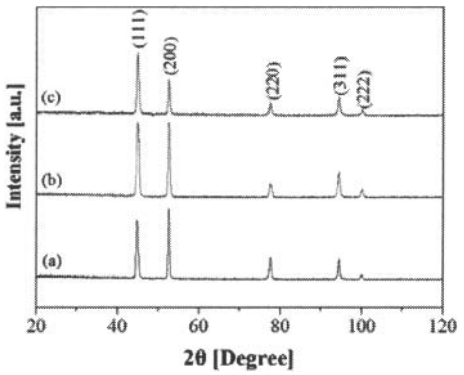

Figure 3. XRD patterns of 2024 aluminium alloy: (a) as-received, (b) rolled with thickness reduction of 50 % at 380 °C and (b) with SMAT and thickness reduction of 50 % at 380 °C.

It is commonly observed that the failure mode for AA2024-T3 sheets is cup-cone rupture (Figure 4b), the fracture characteristics are similar to those ductile materials (Figure 4a). Further investigation on the SMATed specimen has shown the changes from cup-cone rupture to cleavage (Figure 4c). The low-plastic-strain fracture is associated with areas of a shallow dimpled structure and cleavage of the flattened grains in the proximity of some oxide inclusions. This observation indicates the nature of ductile fracture of AA2024-T3 is restricted.

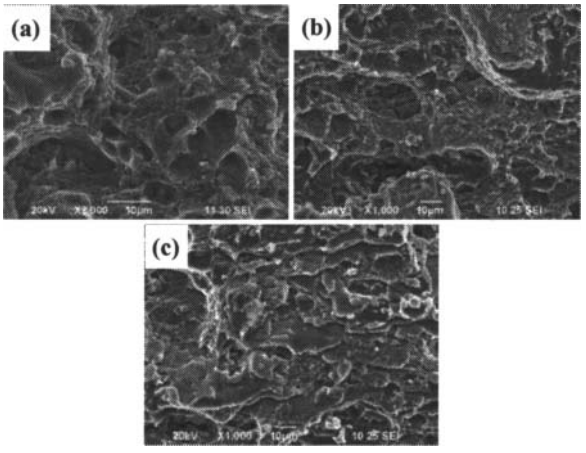

Figure 4. SEM fractographs of AA2024-T3 specimens: (a) as-received, (b) rolled with thickness reduction of 50 % at 380 °C and (c) with SMAT and thickness reduction of 50 % at 380 °C.

Conclusions

The effects of SMAT on mechanical properties of aluminium were studied. Tensile tests were conducted for various materials under different conditions. The ultimate tensile strengths of Al2024 after the SMAT and rolling process improved significantly. To sum up, the results obtained from the tensile tests above demonstrate that, provided the SMAT process for Al2024 was rolling at room temperature and 80% thickness reduction, the sample was shown to exhibit optimised yield and ultimate tensile strength and desirable ductility. The effect of SMAT produced not only the nanostructure layer, but also some compressive stress on the surface layer of the aluminium sheets. The present study suggests that with this combination of enhanced yield and ultimate tensile strength in one material, aluminium alloy could become a strong candidate for utilisation within the aerospace industry. It also may serve to inform future research into the production of high strength alloys for other specific uses.

Acknowledgements

The authors would like to acknowledge the support from the Research Grants Council of Hong Kong Special Administrative Region of China (CityU518907 and CityU8/CRF/08).

References

1. Michael F. Ashby, Materials Selection in Mechanical Design Chapter 6 (Oxford: Pergamon Press, 1992).
2. L. Lu, and J. Lu, "Surface Nanocrystallization (SNC) of Metallic Materials - Presentation of the Concept behind a New Approach," Journal of Materials Science and Technology, 15 (3) (1999), 193-197.
3. K. Lu, and J. Lu, "Nanostructured Surface Layer on Metallic Materials Induced by Surface Mechanical Attrition Treatment," Materials Science and Engineering A - Structural Materials Properties Microstructure and Processing, 375 (2004), 38-45.
4. Y. Wang et al., "Improved Fatigue Behavior of Pipeline Steel Welded Joint by Surface Mechanical Attrition Treatment (SMAT)," Journal of Materials Science and Technology, 25 (4) (2009), 513-515.
5. N.R. Tao et al., "An Investigation of Surface Nanocrystallization Mechanism in Fe Induced by Surface Mechanical Attrition Treatment ," Acta Materialia, 50 (18) (2002), 4603-4616.
6. W.P. Tong et al., "Nitriding Iron at Lower Temperatures," Science, 299 (2003), 686-688.
7. W.P. Tong et al., "The Formation of ε-Fe-3-N-2 Phase in a Nanocrystalline Fe," Scripta Materialia, 50 (2004), 647-650.
8. M.A. Meyers, A. Mishra, and D.J. Benson, "Mechanical Properties of Nanocrystalline Materials," Progress in Materials Science, 51 (2006), 427-556.
9. Z.B. Wang et al., "Diffusion of Chromium in Nanocrystalline Iron Produced by Means of Surface Mechanical Attrition Treatment," Acta Materialia, 51 (2003), 4319-4329.
10. R. Valiev, "Nanostructuring of Metals by Severe Plastic Deformation for Advanced Properties," Nature Materials, 3 (8) (200), 511-516.
11. C.S. Wen et al., "Nanocrystallization and Magnetic Properties of Fe-30 Weight Percent Ni Alloy by Surface Mechanical Attrition Treatment," Metallurgical and Materials Transactions A, 37 (5) (2006), 1413-1421.
12., N.R. Tao et al., "Mechanical and Wear Properties of Nanostructured Surface Layer in Iron Induced by Surface Mechanical Attrition Treatment," Journal of Materials Science & Technology, 19 (6) (2003), 563-566.
13. S. Kweon et al., "Development of Localized Deformation in AA 2024-O," Journal of Engineering Materials and Technology - Transactions of the ASME, 131 (3) (2009), 031009-1-8.
14. N. Tsuji et al., "Ultra-Fine Grained Bulk Steel Produced by Accumulative Roll-Bonding (ARB) Process," Scripta Materialia, 40 (7) (1999), 795-800.
15. N. Tsuji, K. Shiotsuki, and Y. Saito, "Superplasticity of Ultra-Fine Grained Al-Mg Alloy Produced by Accumulative Roll-Bonding," Materials Transactions Jim, 40 (8) (1999), 765-771.

16. S.H. Lee et al., "Strengthening of Sheathrolled Aluminum Based MMC by the ARB Process," Materials Transactions Jim, 40 (12) (1999), 1422-1428.
17. N. Tsuji et al., "Ultra-Fine Grained Ferrous and Aluminum Alloys Produced by Accumulative Roll-Bonding," Ultrafine Grained Materials, ed. R.S. Mishra, S.L. Semiatin, C. Suryanarayana, N. N. Thadhani, and T.C. Lowe, (Warrendale: Minerals, Metals & Materials Society, 2000), 207-218.
18. Y. Ito et al., "Change in Microstructure and Mechanical Properties of Ultra-Fine Grained Aluminum during Annealing," Journal of the Japan Institute of Metals, 64 (6) (2000), 429-437.
19. N. Kamikawa et al., "Quantification of Annealed Microstructures in ARB Processed Aluminium," Acta Materialia, 54 (11) (2006), 3055-3066.
20. M.Z. Quadir et al., "Influence of Processing Parameters on the Bond Toughness of Roll-Bonded Aluminium Strip," Scripta Materialia, 58 (11) (2008), 959-962.
21. S. Malekjani et al., "Cyclic Deformation Response of UFG 2024 Al Alloy," International Journal of Fatigue, 33 (5) (2011), 700-709.
22. S. Cheng et al., "Optimizing the Strength and Ductility of Fine Structured 2024 Al Alloy by Nano-Precipitation," Acta Materialia, 55 (17) (2007), 5822-5832.
23. X. Wu et al., "Strain-Induced Grain Refinement of Cobalt during Surface Mechanical Attrition Treatment," Acta Materialia, 53(3) (2005), 681-691.
24. H.L. Chan, J. Lu, and A. Schoberth, "Study of the Mechanical Properties of Nanostructured Aluminum Obtained by SMAT," ASME Conference Proceedings, IMECE2007-43290, 13 (2007), 39-43.
25. L. Birks, and H. Friedman, "Particle Size Determination from X-Ray Line Broadening," Journal of Applied Physics, 17 (8) (1946), 687-692.
26. T. Ungár, "Microstructural Parameters from X-ray Diffraction Peak Broadening," Scripta Materialia, 51 (8) (2004), 777-781.